The response surface methodology for optimization of tyrosinase immobilization onto electrospun polycaprolactone–chitosan fibers for use in bisphenol A removal

Jakub Zdarta[1*], Maciej Staszak[1], Katarzyna Jankowska[1], Karolina Kaźmierczak[1], Luong N. Nguyen[2], Ewa Kijeńska-Gawrońska[3], Manuel Pinelo[4], Teofil Jesionowski[1]

[1] Institute of Chemical Technology and Engineering, Faculty of Chemical Technology, Poznan University of Technology, Berdychowo 4, PL-60965 Poznan, Poland

[2] Centre for Technology in Water and Wastewater, University of Technology Sydney, Ultimo 2007, New South Wales, Australia

[3] Faculty of Materials Science and Engineering, Warsaw University of Technology, Woloska 141, PL-02507 Warsaw, Poland

[4] Department of Chemical and Biochemical Engineering, Technical University of Denmark, Soltofts Plads, Building 227, DK-2800 Kongens Lyngby, Denmark

* Corresponding author:

Jakub Zdarta, jakub.zdarta@put.poznan.pl,

Abstract

Composite polycaprolactone–chitosan materials were produced by an electrospinning method and used as a support for immobilization of tyrosinase by mixed ionic interactions and hydrogen bonds adsorption. The morphology of the fibers and effective enzyme deposition were confirmed from SEM images. Further, multivariate polynomial regression was used to model the experimental data and determine optimal conditions for the immobilization process, which were found to be pH 7, temperature 25 °C and 16 h process duration. Under these conditions, immobilization yield reached 93% and highly active biocatalytic systems were produced characterized by expressed activity of 95%. These systems were then applied in the biodegradation of bisphenol A under various remediation conditions in a batch system. It was found that after 120 min of the process, in the temperature range 15–45 °C and the pH range 6–9, from solutions at concentrations up to 3 mg/L, over 80% of the pollutant was removed. Furthermore, the stability and reusability of the tyrosinase were significantly improved upon immobilization: the immobilized biomolecule retained around 90% of its initial activity after 30 days of storage, and was capable of removing over 80% of bisphenol A even after 10 repeated uses. By contrast, free enzyme removed over 80% of bisphenol A over pH and temperature range 7–8 and 15–35 °C, respectively and retained less than 60% of its initial activity after 30 days of storage.

Keywords: enzyme immobilization; immobilization optimization; bisphenol A removal

1. Introduction

The widespread use of bisphenols in industry, and their adverse impact on living organisms, including mutagenic and cancerogenic effects, make it essential to monitor their circulation in the environment [1–4]. Many studies are focused on searching for efficient and environmentally friendly methods of degradation of phenolic compounds and their derivatives [5,6]. One of the approaches of particular interest is the biodegradation of toxic pollutants using enzymes: natural biocatalysts having the ability to oxidize phenols, dyes, pharmaceuticals and estrogens [7,8]. The enzymes most widely used in biodegradation are those of the oxidoreductase group, including peroxidases such as horseradish, lignin or chloroperoxidase, and polyphenol oxidases such as laccase and tyrosinase [9–11]. Recently, increased

attention has been paid to tyrosinase, as this enzyme is capable of efficient degradation of phenols and bisphenols by catalytic conversion into corresponding quinones, which tend to form oligomeric and polymeric compounds that can be easily separated from solution by precipitation [12,13]. Mechanism of catalytic action of tyrosinase consist of hydroxylation and subsequent oxidation reaction of phenols into ortho-quinones with simultaneous reduction of oxygen, as a co-substrate, to water. The most commonly used is mushroom *Agaricus bisporus* tyrosinase which was reported to be a glycosylated, tetrameric protein with a molecular mass of around 120 kDa, composed of two heavy subunits of~43 kDa (H subunit) and two lights subunits of ~14 kDa (L subunit) [14,15]. This tyrosinase possesses isoelectric point at pH 4.7–5, whereas shows its maximum activity at pH around 7 and at mild temperature of around 25 °C [16]. In general, tyrosinase consists of three various domains, among which, the central domain, responsible for catalytic action of this enzyme contains two Cu binding sites, called CuA and CuB, which interact with both molecular oxygen and phenolic substrate. Furthermore, the mushroom tyrosinase has 11 cysteine residues at N-terminal domain and 1 cysteine residue at C-terminal domain that stabilize protein structure by internal disulfide linkages [17].

The limited practical application of native enzymes, due to their low activity, poor stability and lack of reusability, can be overcome with the use of immobilization, where the protein is bound to a solid carrier [18,19]. The immobilization of biomolecules provide some operational stability, provide higher resistance against adverse effects of the reaction conditions, as well as facilitate reuse of the enzymes [20]. The retention of catalytic activity and improvement of stabilization is the main goal of the successful immobilization. In this context, a controlled immobilization, particularly using porous supports, might have a positive enzyme on the enzyme maintenance and performance as might reduce diffusional limitations and partitions as well as enzyme aggregation and its inhibition and prevent against internal conformational changes in the enzyme structure [21,22]. Furthermore, immobilization might produce significant enzyme stabilization when enzyme is multipointly immobilized [23], as well as when the favorable environment for the enzyme is generated upon immobilization [24]. A proper immobilization might also lead to enhancement of enzyme catalytic activity under harsh process conditions and over storage time and might improve enzyme selectivity and/or specificity [22]. Finally, examples of enzyme purification by immobilization has been also reported [25,26].

Among others immobilization strategies, adsorption approach based on formation of ionic, hydrogen or mixed interactions, is the most commonly used. This is mainly due to the simplicity of the immobilization procedure, low-cost and usually observed retention of high catalytic activity by the immobilized biomolecules [27,28]. Adsorption immobilization is characterized by low-force interaction, however, physical adsorption of biomacromolecules are multipoint processes [29,30] having advantages and disadvantages. On the one hand, the structure of the enzyme is insensibly altered and there is a possibility to reuse the support [22]. On the other hand, weak interactions might lead to elution of the enzyme from the support that results in fast decrease of catalytic properties and limited reusability [31]. It should be highlighted, that recently, also oxidoreductases have been immobilized by adsorption and other techniques, to improve their properties in environmental applications. For instance, lignin peroxidase immobilized on chitosan was shown to degrade over 95% of textile dyes, and laccase immobilized on nanoporous silica beads was capable for removing over 90% of 2,4-dinitrophenol [32,33]. In another study, tyrosine immobilized on silica alginate was used for the removal of bisphenol A with an efficiency of close to 100% [34].

It is important to note, however, that the success of immobilization is highly dependent on the selection of a suitable carrier, as well as the determination of optimal process conditions, which affect the final parameters of the immobilized enzymes [35,36]. There has been much research in the past decade on the immobilization of enzymes and the selection of optimal carriers. In recent years, electrospun carriers have aroused particular interest, due to the possibility of producing tailor-made materials with high porosity and enzyme affinity [37]. However, bearing in mind the specificity of each enzyme and the individual nature of the process, it is extremely important to select the most favorable conditions for the immobilization of a given protein [38]. Parameters requiring analysis include the pH and temperature of the immobilization process, which may cause inactivation of the biocatalyst, and the process time and initial enzyme concentration, which may affect the quantity of immobilized enzyme and its activity [39]. The one-factor-at-a-time (OFAT) method, response surface methodology (RSM) and Box–Behnken design (BBD) are techniques used for modeling of the immobilization process and selection of the optimal conditions [40,41]. However, methods of data matching have also been used to

optimize enzyme immobilization [42]. The criteria listed above have a great impact on attainment of the maximum enzyme activity and on the possible applications of the immobilized biocatalysts.

Having regard to the limited availability of data on the efficient immobilization of tyrosinase and optimization of that process, in the present study, for the first time, we have attempted to produce novel polycaprolactone–chitosan (PCL–chitosan) electrospun materials and to use them for the immobilization of tyrosinase. The produced PCL–chitosan material, beside relatively good mechanical stability, has a specific surface area of around 70 m^2/g and is characterized by the presence of hydroxyl, amine and carbonyl groups onto its surface. These groups are capable for creation of hydrogen bonds and ionic interactions with functional groups presented in enzyme structure, including mainly amine, hydroxyl and carboxyl moieties during enzyme immobilization process (Fig. 1). Moreover, this support material was selected due to its biocompatibility, open three-dimensional structure, high volume to mass ratio and relatively low-cost of its production. A thorough analysis, including modeling of the immobilization process and optimization of its conditions, was performed to obtain a biocatalytic system offering high catalytic activity. The stability and reusability of the immobilized biomolecules were also examined. Finally, the possible practical application of the produced biocatalytic systems was validated by using them in the biodegradation of bisphenol A under various conditions, to evaluate the influence of these parameters on the efficiency of removal.

Figure 1

2. Materials and Methods

2.1. Chemicals and reagents

Polycaprolactone (PCL) with molecular weight 80 kDa, chitosan with molecular weight 1000 kDa, trifluoroacetic acid (TFA), mushroom tyrosinase (polyphenol oxidase, activity ~2000 U/mg solid, EC 1.14.18.1), 100 mM acetate buffer (pH 3–5), 100 mM phosphate buffer (pH 6–8), 100 mM bicarbonate buffer (pH 9, 10), bisphenol A (BPA) (purity ≥99%) and L-catechol were supplied by Sigma-Aldrich (USA).

2.2. Fabrication of PCL–chitosan materials

To prepare PCL–chitosan electrospun fibers, chitosan was dissolved in TFA to obtain a 5% (w/v) solution and obtained mixture was stirred for 4 h at 75 °C. Polycaprolactone was dissolved in TFA to

obtain a 10% (w/v) solution and was stirred for 4 h at room temperature. The solutions of chitosan and PCL in TFA were combined in the ratio 85:15 (w/w) and were stirred for 1 h. The resulting PCL–chitosan solution was placed in a plastic syringe and electrospun using a NANON-01A device (MECC Co. Ltd., Japan). The applied voltage was set at 20 kV, the distance between nozzle and collector was 150 mm, and the ejection rate was 1 mL/h. The obtained PCL–chitosan fibers were dried in a vacuum drier under vacuum at 25 °C.

2.3. Tyrosinase immobilization

Immobilization of mushroom tyrosinase was performed by adsorption; however, one of the goals of the study was to find the most suitable immobilization conditions, including temperature, process duration, and the pH and concentration of the initial enzyme solution, so as to obtain immobilized enzymes with good catalytic properties. For immobilization, 10 mg of PCL–chitosan material (two pieces of size 1 cm x 1 cm), washed with distilled water, was placed in 10 mL of tyrosinase solution at the desired concentration (from 0.5 to 5.0 mg/mL) prepared in 100 mM buffer solution at an appropriate pH (ranging from 4 to 9). The samples were then placed in a shaker (IKA Werke GmbH, Germany) and were agitated at 150 rpm for a specified period of time ranging from 1 h to 24 h, at various temperatures (from 5 ºC to 55 ºC). After immobilization, samples were separated from the reaction mixture and were washed with 100 mM phosphate buffer at pH 7 to remove unbound enzyme.

2.4. Modeling of the effect of process conditions on the activity of immobilized enzyme

The mathematical model proposed was formulated using Mathcad software. For the six distinct data sets, with different independent variables, the *polyfit* function was used to generate the response surface. Based on the least squares modelhood, the problem of fitting the surface consisted in finding such parameters as defined by equation (1), to obtain the smallest value of the sum of squared distances between data points and the surface. Calculating the partial derivatives of F is straightforward for the formulation chosen, although a numerical procedure might be required in the case of more complex surface functions. In the case presented, symbolic solutions for the optimal parameters A_{opt} and B_{opt} were derived analytically.

2.5. Immobilization yield, enzyme activity and stability

The activity and stability of the free and immobilized enzymes were examined based on a model reaction using L-catechol as a substrate, by measuring the progress of formation of ortho-quinones, according to the methodology presented by Dincer et al. [43] with slight modification. Briefly, for the reaction, 50 mg of free or immobilized tyrosinase was added to 10 mL of 20 mM L-catechol solution in 100 mM phosphate buffer at pH 7. The process was carried out for 60 min at 25 ºC with a continuous oxygen supply with a flow rate 1 mL/min. One unit of free and immobilized tyrosinase activity was defined as the amount of enzyme that liberates 1 mM of ortho-quinones per minute under assay conditions. Based on the results, the activity retention of the immobilized enzymes was calculated and presented as the percentage activity of the immobilized laccase as compared to the catalytic activity of free enzyme. For the study of storage and thermal stability, the initial value of enzyme relative activity was defined as 100% activity.

The storage stability of the free and immobilized tyrosinase was examined by spectrophotometric measurements, based on the above model reaction using L-catechol as substrate, over 20 days of storage at 4 ºC in 100 mM phosphate buffer at pH 7. Measurements of relative activity were performed at regular time intervals.

The thermochemical stability of the free and immobilized enzymes was determined over 120 min of incubation under optimal temperature and pH conditions (25 ºC and pH 7), based on the reaction using 20 mM L-catechol as a substrate. Spectrophotometric measurements were made after a specified heating time, to calculate the relative activity. In addition, inactivation parameters of the free and immobilized enzymes—the inactivation constant (k_D) and enzyme half-life ($t_{1/2}$)—were calculated based on the linear regression slope of inactivation curves.

The immobilization yield and expressed activity was calculated following to eq. 1 and eq. 2:

$$Immobilization\ yield\ (\%) = \frac{A_i - A_f}{A_i} \cdot 100\% \qquad \text{(eq. 1)}$$

$$Activity\ recovery\ (\%) = \frac{A_t}{A_i} \cdot 100\% \qquad \text{(eq. 2)}$$

where: A_i denotes the initial activity of the tyrosinase added to the immobilization medium, A_f denotes the total activity of the enzyme in the supernatant and washing solution after the immobilization and A_t

denotes the activity of the immobilized tyrosinase. The activities of the supernatant and reference samples were determined under standard conditions, based on the above-presented reaction.

The kinetic parameters of the free and immobilized tyrosinase—the Michaelis–Menten constant (K_m) and maximum reaction rate (V_{max})—were determined against L-catechol as a substrate, by measuring initial reaction rates, based on the above-mentioned reaction of L-catechol oxidation under optimal process conditions with a continuous oxygen supply with a flow rate 1 mL/min, using various substrate solutions at concentrations from 0.5 to 20 mM. The apparent kinetic parameters of free and immobilized tyrosinase (K_m and V_{max}) were calculated using Hanes–Woolf plot.

2.6. Removal of bisphenol A

Degradation of BPA by free and immobilized tyrosinase was performed using an IKA KS 4000i Control incubator (IKA Werke GmbH, Germany). For the BPA removal experiments, to a BPA solution at desired concentration, 10 mg of free or immobilized enzyme was added. The samples were mixed under specified process conditions at 150 rpm for 120 min with a continuous oxygen supply with a flow rate 1 mL/min, and were analyzed at specified intervals to determine the BPA removal rate over time.

The effect of initial BPA concentration on the removal rate was examined using solutions at concentrations 0.1, 0.5, 1.0, 3.0 and 5 mg/L at pH 7 and 25 ºC. The effect of pH on the removal rate of bisphenol A was examined over a wide pH range from 3 to 10, using 100 mM buffer solutions at appropriate pH to adjust the pH value. The process was performed at 25 ºC using BPA solution at concentration 3 mg/L. To assess the effect of temperature on the removal of BPA, biodegradation was performed at temperatures from 5 ºC to 65 ºC (with a 10 ºC step) using BPA solution at concentration 3 mg/L at pH 7.

The reusability of the immobilized tyrosinase was examined over ten repeated cycles of bisphenol A removal. Briefly, each cycle was performed over 120 min at 25 ºC using a solution at pH 7 with an initial BPA concentration of 3 mg/L. After each biodegradation step, the immobilized tyrosinase was separated from the reaction mixture, washed several times with 100 mM phosphate buffer at pH 7, and placed in a fresh BPA solution.

2.7. Analytical techniques

The morphology of the fabricated PCL–chitosan electrospun fibers before and after tyrosinase immobilization was described from SEM photos (EVO40, Zeiss, Germany). The average diameters of the obtained fibers before and after enzyme attachment were calculated using the Image J program (National Institute of Health, USA).

The efficiency of removal of bisphenol A, as well as the stability and reusability of the free and immobilized enzyme, were determined based on spectrophotometric measurements using a Jasco V-750 spectrophotometer (Jasco, Japan), measuring the absorbance during ABTS oxidation at wavelength 420 nm (stability study) and during BPA removal at λ=480 nm. The final concentration of ortho-quinones after the oxidation process, and the concentration of BPA after biodegradation, were obtained based on calibration curves for ortho-quinones and BPA respectively. The efficiency of removal of bisphenol A (%) was calculated by considering the initial and the final concentration of the pollutant in the solution before and after degradation under specified conditions.

2.8. Statistical analysis

All experiments and measurements were performed in triplicate, and error values are presented as means ± standard deviation. Statistically significant differences were determined by one-way ANOVA using Tukey's test, performed in SigmaPlot 12 software (Systat Software Inc., USA). Statistical significance was established at a level of $p<0.05$.

3. Results and Discussion

3.1. Morphological characterization of fibers before and after immobilization

In the first stage of the investigation, in order to characterize the morphological structure of the obtained materials and confirm effective enzyme immobilization, SEM images were made of the PCL–chitosan electrospun fibers before and after tyrosinase immobilization (Fig. 2). It can be seen that the electrospun fibers before attachment of tyrosinase (Fig. 2a) are branched, with a smooth surface, and have an average diameter of 344 ± 121 nm. By contrast, after enzyme deposition a significant increase in fiber diameter (average diameters of 689 ± 365 nm) was observed, indicating attachment of the enzyme on the surface of the fibers. Mushroom tyrosinase is characterized by the molecular weight of around 120 kDa thus,

irregular shapes almost uniformly covered surface of the fibers (Fig. 2b) confirms effective enzyme immobilization and suggests formation of aggregates of immobilized enzyme [44]. This might lead to the occurrence of partition and diffusional problems upon immobilization that reduce enzyme activity. However, it should be noted that the electrospun material has a multidimensional structure with relatively large pores of irregular shape and size, which reduce diffusional resistance and facilitate efficient transport of reaction substrates and products between active centers of the immobilized enzyme and the reaction mixture [45]; this makes the obtained material a suitable support for the immobilization of biomolecules.

3.2. Modeling of the effect of process conditions on the activity of immobilized enzyme

As one the most important objectives of the study was to produce highly active biocatalytic systems for the removal of pollutants, the proper selection of immobilization parameters, including initial enzyme solution concentration, pH and process duration, is crucial. Therefore, in this study, the effect of process conditions on the activity of immobilized tyrosinase was modeled in order to determine the optimal process parameters.

The technique of response surface methodology was used, leading to a model that serves to find the optimum immobilization conditions. Additionally, for the pH and the time of the process t, the influence of other parameters such as temperature T, initial concentration of enzyme solution C, and their relations with catalyst activity were estimated and analyzed. The analysis consisted in selecting an appropriate multidimensional function $F(A, B)$ exhibiting a similar character to the data measured; see equation (1). The usual measure of the quality of fit of a model and data variance is standard deviation. It is important that the mathematical model describing the data should not be too complex, to prevent overfitting and consequently to avoid identifying false trends. The model must also not be too simple, so that it reflects all of the relevant relationships in the measured results. The choice of the order of multivariate polynomial F in the form given by equation (1) is justified by the fact that for higher, even third-degree formulations the resultant models exhibit several extrema, which cannot be explained by the measured data variance. Besides, the existence of several maxima and saddle points in the model makes the problem more difficult to solve. Numerous extrema which might exist in a model fitted to data will always lead to problems regarding the localness of the optimum; for example, the results

obtained might not reflect a global optimum for the process parameters. Moreover, mathematical solution of the optimum search problem stated in terms of higher-order polynomials becomes impossible by analytical methods, and can only be done by a numerical approach, which should be avoided if possible due to the greater complexity involved. The higher quality of fit obtainable using polynomials of higher degree than two does not compensate for the risk of obtaining false positive optimization results.

For each model presented, the calculated value of standard deviation describes the amount of variation in the data that is not explained by the model; the lower this value, the better. The model's quality of fit is also indicated by the value of the determination coefficient R^2. This indicates the fraction (or percentage) of the total variance of the data that is explained by the model; the closer this value is to 1 (or 100%), the better. The data fit procedure utilizes linear statistical estimation to obtain a nonlinear model of the dependence of activity on selected explanatory variables *A* and *B*. The explanatory variables *A* and *B* may denote pH, process time, temperature or concentration, according to the analysis selected.

$$F(A,B) = a_1 + a_2 A + a_3 B + a_4 A \cdot B + a_5 A^2 + a_6 B^2 \quad (1)$$

The response surface methodology is implemented on the continuous domain over which the fitted model is defined, by applying partial derivative operators to a model mathematical function. The partial derivatives of model *F* are given by:

$$\frac{dF}{dA} = a_2 + a_4 B + 2a_5 A \quad (2)$$

$$\frac{dF}{dB} = a_3 + a_4 A + 2a_6 B \quad (3)$$

The resultant formulations for the analytical solution of equations obtained by setting the expressions in (2) and (3) equal to zero can be solved analytically, representing the optimization problem defined in terms of surface response methodology. The solutions to the problem are given by equations (4) and (5).

$$A_{opt} = \frac{-a_3 a_4 + 2a_6 a_2}{a_4^2 - 4a_5 a_6} \quad (4)$$

$$B_{opt} = -\frac{a_4 a_2 - 2a_5 a_3}{a_4^2 - 4a_5 a_6} \qquad (5)$$

The advantage of the response surface methodology optimization presented in the analytical form of solutions (4) and (5) is that it is general in the sense of the model used, and does not require a numerical approach to find the optimal process conditions. It is important to note, however, that this solution is tailored only to the model F presented in (1).

A typical view of the response surface, based on the pH–process time model for catalyst activity, is shown in Fig. 3. The model F exhibits only one global maximum, which is justified by observing the measured experimental data. The response surface is a statistical fit, and it therefore extends far beyond the experimental values, in the range $(-\infty, \infty)$. The meaningful range of F is located inside the convex hull containing experimental data points. Although the formal convex hull is not calculated here, it can easily be estimated by examining the minimum and maximum values of the measured data, that is, the explanatory (A and B) variables. Only within this range and in its close neighborhood can the response surface exhibit physically meaningful results.

Figure 3

The detailed results obtained by calculation are given in Table 1. Six distinct sets of experimental values were used, which relate selected independent variables A and B to the measured activity of the catalyst. The actual process variables denoted by A and B are given in the first two columns.

Table 1

The values a_i represent the coefficients of a model F for a given relation between variables that affect the catalyst's activity. Their meaning is statistical only, and they have no physical significance. Nonetheless, they play a key role in the model formulation. The optimal values A_{opt} and B_{opt} for process parameters represent the results from the response surface analysis. These provide the values of process parameters—pH, time t, concentration C, and temperature T—that lead to the highest activity of the catalyst. The quality of the models is confirmed by high values of the determination coefficient R^2, close to one, and relatively low values of the standard deviation in comparison to the activity values.

3.3. Characterization of immobilized enzyme

Based on the result of modelling study and preliminary experiments, immobilization conditions allowing obtaining of immobilized tyrosinase with the highest catalytic activity were found to be: pH 7, temperature 25 °C, initial enzyme concentration 3 mg/mL and 16 h of immobilization duration. Under these conditions, immobilization yield reached 93% and 95% of activity recovery was attained. Slight decrease in enzyme activity, as compared to free counterpart, might be related to the formation of diffusional limitation in transport of L-catechol and oxygen and products upon immobilization [46] as well as some distortion of enzyme structure due to its binding to the support [21]. Nevertheless, high catalytic activity was retained in the support after tyrosinase immobilization [47]. Immobilized tyrosinase obtained under process conditions differ than optimal showed lower activity recovery due to negative effect of the process conditions on enzyme structure and its activity. As produced immobilized tyrosinase is also characterized by the highest stability among all systems produced and tested at various immobilization conditions. It should be noted that enzyme loading, beside influence on enzyme activity [48], might also affect its stability due to possible changes in the distances of enzyme-support interactions in a highly-loaded enzymatic systems [49]. It has been reported that high immobilization yield, corresponds with high enzyme loading, leads to improve in enzyme stability due to crowding formation and reduction of enzyme mobility [50,51]. On the other hand, internal hydrophobic enzyme interactions as well as enzyme-enzyme interactions in the highly loaded support lead to the irreversible conformational changes leading to the drop in enzyme activity [52]. Furthermore, the occurrence of diffusional limitations in highly loaded immobilized enzymes cause that apparent activity of these enzymes is higher, as compared to the systems where diffusional restrictions did not occur [53]. In addition, to follow the immobilization progress an immobilization curve was plotted under optimal immobilization conditions (Fig. 4). It can be seen that enzyme-support reaction is not very intense as after 3 h less than 40% of the activity was immobilized. This might be due to the homogenous distribution of support functional groups onto its surface [54]. Progress in the immobilization duration leads to decrease of residual activity of supernatant. After 16 h of process time most of the enzyme activity was immobilized and expressed activity of the immobilized tyrosinase reached 95%.

Prolongation of the immobilization increased supernatant residual activity probably due to enzyme leaching from the support.

Figure 4.

3.4. Removal of Bisphenol A

Free tyrosinase and the immobilized system produced under optimal immobilization conditions and exhibiting the highest catalytic properties were further applied and compared in the removal of bisphenol A from water solution under various remediation conditions. Immobilized tyrosinase was used in this study because this enzyme is capable of efficient degradation/conversion of mono- and bisphenols [55], and because biomolecules deposited on solid carriers, unlike free enzymes, offer improved resistance against inactivation by harsh process conditions and can be easily separated from reaction mixtures [56], which is of great importance for the treatment of large volumes of polluted wastewater.

Figure 5a shows the percentage removal of bisphenol A by the free and immobilized enzyme over time. It can be seen that irrespective of the biocatalyst used, removal efficiency increased gradually over the initial stage of the process, reaching 100% after 60 min and 90 min of the process in the case of free and immobilized tyrosinase respectively. Nevertheless, over the whole analyzed period, the immobilized biomolecules produced a slightly lower removal rate than the free enzyme, which may be due to the lower activity of PCL–chitosan-bonded tyrosinase (an activity recovery of 95%) and accumulation of the products of enzymatic conversion, leading to inhibition of the biocatalyst [57]. Furthermore, the results obtained are in agreement with the data for the kinetic parameters obtained using L-catechol as a substrate. The values of the Michaelis–Menten constant (K_m) for the free and immobilized enzyme were 1.46 mM and 2.53 mM respectively, indicating the lower substrate affinity of tyrosinase after immobilization. Moreover, the maximum velocity rate (V_{max}) of the free enzyme (46.8 U/mg) was higher than the V_{max} of the immobilized enzyme (31.4 U/mg). The lower substrate affinity of immobilized enzyme might be explained by the formation of diffusional limitations upon immobilization due to partial blocking of enzyme active sites and aggregation of tyrosinase molecules [58]. The changes in the values of the kinetic parameters upon immobilization are also attributed to the fact that the immobilized enzyme is located in an environment different from that of its free form, leading to alterations in its microenvironment and causing changes in the enzyme kinetics. Furthermore,

change in the substrate affinity might be related to the structural changes in enzyme structure and formed in enzyme-support interactions [59,60]. Similar observations were made by Dincer et al. (2012), who immobilized tyrosinase onto chitosan–clay composite beads and noticed high activity retention accompanied by pronounced changes in enzyme kinetic. Two times lower substrate affinity and 40% lower V_{max} value of the immobilized tyrosinase were explained by diffusional limitations, steric effects and alteration of enzyme structure [43].

In the following steps, we investigated the effect of various process parameters on process efficiency. As bisphenol A is commonly used as an additive and intermediate product in polymer processing, it frequently occurs in wastewaters at various concentrations [61]. Therefore, we decided to examine the rate of removal of BPA over a wide range of concentrations, from 0.1 mg/L to 5 mg/L (Fig. 5b). It is evident that after 120 min of the process, both free and immobilized tyrosinase demonstrated excellent catalytic efficiency, as BPA was totally removed from the solution at concentrations up to 3 mg/L. In the case of the solution at the highest concentration (5 mg/L) a drop in the total removal rate of bisphenol A was recorded. Although higher reaction rate by the immobilized tyrosinase was attained, as compared to the enzyme action in lower BPA concentrations, the 5 mg/L concentration was to high to be fully converted by the enzyme. Furthermore, some distortions of the enzyme structure by the such high substrate concentration might lead to the production of semiinextitated forms that also removal efficiency of bisphenol A. Nevertheless, even from the 5 mg/L solution, over 80% of the BPA was removed from the solution by PCL–chitosan immobilized tyrosinase, indicating the possible practical application of the produced biocatalytic systems for the removal of bisphenols from wastewaters. For comparison, in our previous study on the immobilization of laccase onto spongin-based scaffolds, we demonstrated that the immobilized enzyme was capable of removing over 95% of bisphenol A from water solution at concentration 2 mg/L after 24 h of the treatment process [62].

Another important parameter strongly influencing the stability and catalytic properties of biocatalysts is the temperature of the process. The effect of this parameter on the rate of removal of BPA was investigated over a temperature range from 5 °C to 65 °C (Fig. 5c). As shown, the optimum process temperature, for both free and immobilized enzyme, was found to be 25 °C, as in these conditions total removal of bisphenol A occurred. A change in temperature to higher or lower values led to a significant

drop in the rate of removal of the pollutant by the free enzyme. By contrast, immobilized tyrosinase exhibited high activity over a wider temperature range; it removed over 80% of BPA at temperatures ranging from 15 °C to 55 °C. Even at 65 °C around 70% of the bisphenol was converted by the immobilized biomolecules, over 30% more than in the case of removal by the free enzyme. This clearly demonstrates that the immobilized enzyme due to protection against thermal inactivation was more stable as its free counterpart, even at higher temperatures. The improvement in the enzyme's stability against harsh temperature conditions upon immobilization might be explained by the formation of enzyme–support interactions which stabilize the structure of the biomolecules, as well as rigidization of the enzyme, which facilitates its application at higher operational temperatures [63,64]. Similar observations have been reported by Tamura et al. [65] and Nicolucci et al. [66], who immobilized tyrosinase using ion-exchange resins and polyacrylonitrile beads, for use in the removal, respectively, of alkylphenols and bisphenol A. Irrespective of the type of support material used, due to enzyme stabilization upon immobilization, the pollutants were removed more efficiently over a wider temperature range by the immobilized tyrosinase than by the free enzyme in solution.

Another key parameter affecting the catalytic activity of biomolecules is pH. We investigated the effect of pH on the rate of removal of BPA over the pH range 3–10 (Fig. 5d). As the diagram shows, pH 7 was found to be the optimum value for both free and immobilized tyrosinase; this is in agreement with previous studies on the application and immobilization of mushroom tyrosinase [67,68]. Beyond this value BPA removal by the free enzyme gradually decreased: only at pH 7 and 8 did it remove more than 80% of the pollutant. By contrast, immobilized tyrosinase displayed improved stability over the whole analyzed pH range. Furthermore, PCL–chitosan-bonded tyrosinase exhibited a less pronounced decline in the BPA removal rate under harsh pH conditions, and enabled the removal of over 80% of bisphenol A in the pH range from 6 to 9. The improvement in the activity of tyrosinase upon immobilization over a wide pH range is attributed to the stabilization of the enzyme structure and protection of the biomolecules against the dissociation of amino acids caused by adverse effects of acidic and basic conditions (H^+ and OH^- ions) [69]. Similar observations have been reported by Wu et al. [70], who immobilized tyrosinase on polyacrylonitrile beads and used them in the biodegradation of phenol. They observed an improvement in enzyme stability over a pH range from 6 to 9; however, total removal

of the phenol was not achieved, indicating the higher capability of the biocatalytic system obtained in this study in the removal of phenolic compounds under various pH conditions.

Figure 5

3.5. Stability and reusability of free and immobilized tyrosinase

It has been reported that immobilization improves the stability of enzymes and facilitates their reuse [7,36]. As thermochemical and storage stability, as well as reusability, are among the key criteria affecting the practical application of immobilized enzymes, we examined and compared these parameters for free and PCL–chitosan-immobilized tyrosinase (Fig. 6).

The free and immobilized biocatalysts were stored at 4 °C over 20 days, and the storage stability was examined at specified time intervals. As shown in Fig. 6a, the free tyrosinase gradually lost its activity during storage, and after 20 days of the test retained less than 50% of its initial activity. As expected, the decrease in the activity of the immobilized enzyme was less marked. Over 5 days of storage no activity loss was observed, and after 20 days of storage PCL–chitosan-immobilized tyrosinase retained over 85% of its initial activity. Although loss of enzymatic activity is a naturally occurring phenomenon, the present data clearly indicate that upon immobilization of tyrosinase on PCL–chitosan electrospun fibers, because of the stabilization of the enzyme structure and multiple enzyme attachment [71], this effect might be effectively reduced. Similar observations have been reported in other studies on the immobilization of various polyphenol oxidases on chitosan-based materials, indicating the positive effect of chitosan on enzyme stability [34,72,73].

Evaluation of the thermochemical stability of an immobilized enzyme over time under process conditions is one of the most important criteria to be considered. In this study we examined and compared the stability of free and immobilized tyrosinase over 120 min of a process carried out at pH 7 and 25 °C (Fig 6b). The relative activities of both the free and immobilized enzyme declined over time, and after 60 min of incubation reached 70% and 85% respectively. Prolongation of the incubation time led to a further drop in relative activity; however, a significantly smaller decrease was observed for immobilized tyrosinase. After 120 min of the test the relative activity of the free enzyme was around 40%, while PCL–chitosan-bonded tyrosinase retained over 80% of its activity. The drop in catalytic activity may be attributed to changes in the tertiary structure of the enzyme caused by the reaction

environment [74]. Nevertheless, the enzyme's thermal stability improved significantly upon immobilization. These results correspond with the values of the inactivation parameters. The inactivation constant (k_d) and half-life ($t_{1/2}$) of free tyrosinase were measured at 0.0083 1/min and 84.5 min. In the case of the immobilized enzyme the inactivation constant and half-life improved more than fivefold compared with free tyrosinase, taking values of 0.0015 1/min and 462 min. The high thermal stability of the immobilized tyrosinase may be explained by several factors, including stiffening of the enzyme structure upon immobilization [75], its protection against distortion and conformational changes of the amino acids in the enzyme structure [76], and the protective effect of the support material against process conditions [77]. All of these factors facilitate the retention of high catalytic properties by the immobilized enzyme [78] and improve its thermal stability.

The reusability of immobilized enzymes over repeated reaction cycles is the most important parameter affecting their practical application, as it can provide advantages—including cost reductions—for treatment processes. Thus, we tested the reusability of the PCL–chitosan-immobilized tyrosinase over ten repeated cycles of bisphenol A removal under optimal process conditions (Fig. 6c). It is seen that the efficiency of removal of BPA slightly decreased with repeated use, and reached approximately 90% after five reaction cycles. The decline in the removal efficiency is related mainly to inhibition of the enzyme by the macromolecular products of catalytic conversion, although because of the adsorption interaction, partial enzyme elution should not be excluded [79]. Nevertheless, it should be highlighted that PCL–chitosan-immobilized tyrosinase exhibits good reusability, as even after ten repeated uses, the biocatalytic system removed over 80% of the BPA. The maintenance of high rates of BPA removal by immobilized tyrosinase over numerous treatment steps is attributed mainly to the stabilization of the enzyme structure, and improvement of its durability under reaction conditions that facilitate the retention of catalytic activity, as previously reported [80,81]. Similar conclusions were reached by Veismoradi et al. [82] and Wu et al. [70], who immobilized tyrosinase using polyaniline membrane coated with chitosan, and polyacrylonitrile beads. The biocatalytic systems were used for the removal of azo dyes and phenols over repeated cycles, and because of the stabilization of the enzyme upon immobilization, attained pollutant removal rates of 80% and 60% respectively after ten repeated uses.

Figure 6

4. Conclusions

Based on the data presented, it can be concluded that PCL–chitosan electrospun composite material is well-suited for the efficient immobilization of mushroom tyrosinase. Data modeling has been applied to determine the optimal immobilization conditions. Multivariate regression analysis based on the least squares method provided values of polynomial coefficients which produced the statistical best fit to the experimental values, and gave a process duration of 16 h at pH 7 and temperature 25 ºC as the optimal process conditions. The produced biocatalytic systems were further applied in a study of the biodegradation of bisphenol A, which showed that the PCL–chitosan-immobilized laccase was capable of achieving total removal of the pollutant over a significantly wider range of pH and temperature than the free enzyme, clearly indicating improvement of the stability of the enzyme upon immobilization. Furthermore, the reusability and stability of the immobilized biomolecules over time were also enhanced. The high stability and reusability of immobilized tyrosinase provide economic advantages for large-scale practical applications of the produced systems, as the high biodegradation rate of bisphenol A suggests that the obtained immobilized enzyme may be considered as a promising tool for the removal of hazardous compounds from water solutions. Moreover, the obtained electrospun PCL–chitosan material may be a promising alternative to synthetic and natural polymers as supports in enzyme immobilization; however, further study is still required.

Acknowledgements: This work was supported by the Ministry of Science and Higher Education (Poland).

References

[1] M.Y. Chen, M. Ike, M. Fujita, Acute toxicity, mutagenicity, and estrogenicity of bisphenol A and other bisphenols, Environ. Toxicol. 17 (2002) 80-86. https://doi.org/10.1002/tox.10035.

[2] S. Kitamura, T. Suzuki, S. Sanoh, R. Kohta, N. Jinno, K. Sugihara, S. Yoshihara, N. Fujimoto H. Watanabe, S. Ohta, Comparative study of the endocrine-disrupting activity of bisphenol A and 19 related compounds, Toxicol. Sci. 84 (2005) 249-259. https://doi.org/10.1093/toxsci/kfi074.

[3] S. Eladak, T. Grisin, D. Moison, M.J. Guerquin, T. N'Tumba–Byn, S. Pozzi–Gaudin, A. Benachi, G. Livera, V. Rouiller–Fabre, R. Habert, A new chapter in the bisphenol A story: bisphenol S and bisphenol F are not safe alternatives to this compound, Fertil. Steril. 103 (2015) 11-21. https://doi.org/10.1016/j.fertnstert.2014.11.005.

[4] J.M. Di Donato, G. Cernera, P. Giovannelli, G. Galasso, A. Bilancio, A. Migliaccio, G. Castoria, Recent advances on bisphenol-A and endocrine disruptor effect on human prostate cancer, Mol. Cell. Endocrinol. 457 (2017) 35-42. https://doi.org/10.1016/j.mce.2017.02.045.

[5] D.P. Mohapatra, S.K. Brar, R.D Tyagi, R.Y. Surampalli, Physico – chemical pretreatment and biotransformation of wastewater and wastewater Sludge – Fate of bisphenol A, Chemosphere 78 (2010) 923-941. https://doi.org/10.1016/j.chemosphere.2009.12.053.

[6] V.A. Angelini, J. Orejas, M.I. Medina, E. Agostini, Scale up of 2,4– dichlorophenol removal from aqueous solutions using Brassica napus hairy roots, J. Hazard. Mater. 185 (2011) 269-274. https://doi.org/10.1016/j.jhazmat.2010.09.028.

[7] J. Zdarta, A. S. Meyer, T. Jesionowski, M. Pinelo, Developments in support materials for immobilization of oxidoreductases: A comprehensive review, Adv. Colloid. Interface. Sci. 258 (2018) 1-20. https://doi.org/10.1016/j.cis.2018.07.004.

[8] K. Chang, T. Teng, Ch. Fu, Ch. Liu, Improving biodegradation of bisphenol A by immobilization and inducer, Process Saf. Environ. Prot. 128 (2019) 128-134. https://doi.org/10.1016/j.psep.2019.05.038.

[9] A. Dwevedi, Enzyme immobilization: Solution towards various environmental issues. Enzyme Immobilization (2016), 87-106. https://doi.org/10.1007/978-3-319-41418-8_5.

[10] V. Aranganathan, C. Kavya, M. S. Sheeja, C. Yuvraj, Construction of biosensor for detection of phenolic compound using thermostabilized Agaricus bisporus Tyrosinase, Arab. J. Sci. Eng. 42 (2017) 11-18. https://doi.org/10.1007/s13369-016-2044-3.

[11] T. Senthivelan, J. Kanagaraj, R. Panda, Recent trends in fungal laccase for various industrial applications: an eco-friendly approach – A review, Biotechnol. Bioproc. 21 (2016) 19-38. https://doi.org/10.1007/s12257-015-0278-7.

[12] G. Faccio, K. Kruus, M. Saloheimo, L. Thöny-Meyer, Bacterial tyrosinases and their applications, Process Biochem. 47 (2012) 1749-1760. https://doi.org/10.1016/j.procbio.2012.08.018.

[13] M. Bilal, M.N. Hafiz, D.B. Iqbal, Mitigation of bisphenol A using an array of laccase-based robust bio-catalytic cues – A review, Sci. Total. Environ. 689 (2019) 160-177. https://doi.org/10.1016/j.scitotenv.2019.06.403.

[14] T-S. Chang, An updated review of tyrosinase inhibitors, Int. J. Mol. Sci. 10 (2009) 2440-2475. https://doi.org/10.3390/ijms10062440.

[15] S. Zolghadri, A. Bahrami, M.T.H. Khan, J. Munoz-Munoz, F. Garcia-Molina, F. Garcia-Canovas, A.A. Saboury, A comprehensive review on tyrosinase inhibitors, J. Enzym. Inhib. Med. Ch. 34 (2019) 297-309. https://doi.org/10.1080/14756366.2018.1545767.

[16] M.E. Marin-Zamora, F. Rojas-Melgarejo, F. Garcia-Canovas, P.A. Garcia-Ruiz, Cinnamic ester of D-sorbitol for immobilization of muschroom tyrosinase, J. Chem. Technol. Biotechnol. 80 (2005) 1356-1364. https://doi.org/10.1002/jctb.1334.

[17] S-Y. Seo, V.K. Sharma, N. Sharma, Muschroom tyrosinase: Recent prospects, J. Agric. Food Chem. 51 (2003) 2837-2853. https://doi.org/10.1021/jf020826f.

[18] A. Roger, S. van Pelt, Enzyme immobilisation in biocatalysis: why, what and how? Chem. Soc. Rev. 42 (2013) 6223-6235. https://doi.org/10.1039/C3CS60075K.

[19] U. Hanefeld, L. Cao, E. Magner, Enzyme immobilisation: fundamentals and application, Chem. Soc. Rev. 42 (2013) 6211-6212. https://doi.org/10.1039/C3CS90042H.

[20] Y. Zhang, J. Ge, Z. Liu, Enhanced activity of immobilized or chemically modified enzymes, ACS Catal. 5 (2015) 4503-4513. https://doi.org/10.1021/acscatal.5b00996.

[21] R.C. Rodrigues, C. Ortiz, A. Berenguer-Murcia, R. Torres, R. Fernandez-Lafuente, Modifying enzyme activity and selectivity by immobilization, Chem. Soc. Rev. 42 (2013) 6290-6307. https://doi.org/10.1039/C2CS35231A.

[22] C. Mateo, J.M. Palomo, G. Fernandez-Lorente, J.M. Guisan, R. Fernandez-Lafuente, Improvement of enzyme activity, stability and selectivity via immobilization techniques, Enzyme Microb. Technol. 40 (2007) 1451-1463. https://doi.org/10.1016/j.enzmictec.2007.01.018.

[23] C. Mateo, O. Abian, R. Fernandez-Lafuente, J.M. Guisan, Increase in conformational stability of enzymes immobilized on epoxy-activated supports by favoring additional multipoint covalent attachment, Enzyme Microb. Technol. 26 (2000) 509-515. https://doi.org/10.1016/S0141-0229(99)00188-X.

[24] C. Garcia-Galan, A. Berenguer-Murcia, R. Fernandez-Lafuente, R.C. Rodrigues, Potential of different enzyme immobilization strategies to improve enzyme performance, Adv. Synth. Catal. 353 (2011) 2885-2904. https://doi.org/10.1002/adsc.201100534.

[25] A.A. Khan, S. Akhtar, Q. Husain, Simultaneous purification and immobilization of mushroom tyrosinase on an immunoaffinity support, Process Biochem. 40 (2005) 2379-2386. https://doi.org/10.1016/j.procbio.2004.09.020.

[26] S. Akhtar, A.A. Khan, Q. Husain, Simultaneous purification and immobilization of bitter gourd (*Momordica charantia*) peroxidases on bioaffinity support, J. Chem. Technol. Biotechnol. 80 (2005) 198-205. https://doi.org/10.1002/jctb.1179.

[27] M.M. Ferreira, F.L.B. Santiago, N.A.G. DaSilva, J.H.H. Luiz, R. Fernandez-Lafuente, A.A. Mendes, D.B. Hirata, Different strategies to immobilize lipase from *Geotrichum candidum*: Kinetic and thermodynamic studies, Process Biochem. 67 (2018) 55-63. https://doi.org/10.1016/j.procbio.2018.01.028.

[28] Y. Lokha, S. Arana-Pena, N.S. Rios, C. Mendez-Sanches, L.R.B. Goncalves, F. Lopez-Gallego, R. Fernandez-Lafuente, 2020. Modulating the properties of the lipase from *Thermomyces lanuginosus* immobilized on octyl agarose beads by altering the immobilization conditions. Enzyme Microb. Technol. 133, 109461. https://doi.org/10.1016/j.enzmictec.2019.109461.

[29] J.M. Bolivar, C. Mateo, J. Rocha-Martin, F. Cava, J. Bernguer, R. Fernandez-Lafuente, J.M. Guisan, The adsorption of multimeric enzymes on very lowly activated supports involves more enzyme subunits: Stabilization of a glutamate dehydrogenase from Thermus thermophilus by immobilization on heterofunctional supports, Enzyme Microb. Technol. 44 (2009) 139-144. https://doi.org/10.1016/j.enzmictec.2008.10.004.

[30] Z. Cabrera, G. Fernandez-Lorente, R. Fernandez-Lafuente, J.M. Palomo, J. M. Guisan, Novozym 435 displays very different selectivity compared to lipase from *Candida antarctica* B adsorbed on other hydrophobic supports, J. Mol. Catal. B Enzym. 57 (2009) 171-176. https://doi.org/10.1016/j.molcatb.2008.08.012.

[31] M. Saleemuddin, Bioaffinity based immobilization of enzymes, in: P.K. Bhatia (Eds.), Thermal biosensors, bioactivity, bioaffinity. Advances in biochemical engineering/biotechnology, Heidelberg, Springer, Berlin, 2001, pp. 203-226. https://doi.org/10.1007/3-540-49811-7_6.

[32] P. Sofia, M. Asgher, M.Shahid, M. A. Randhawa, Chitosan beads immobilized Schizophyllum commune IBL-06 lignin peroxidase with novel thermo stability, catalytic and dye removal properties, J. Anim. Plant Sci. 5 (2016) 1451-1463.

[33] E. Dehghanifard, A. J. Jafari, R. R. Kalantary, A. H. Mahvi, M. A. Faramarzi, A. Esrafili, 2013. Biodegradation of 2,4-dinitrophenol with laccase immobilized on nano-porous silica beads. J. Environ. Health. Sci. Engineer 10, e25. https://doi.org/10.1186/1735-2746-10-25.

[34] M. Kampmann, S. Boll, J. Kossuch, J. Bielecki, S.Uhl, B. Kleiner, R. Wichmann, Efficient immobilization of mushroom tyrosinase utilizing whole cells from Agaricus bisporus and its application for degradation of bisphenol A, Water Res. 57 (2014) 295-303. https://doi.org/10.1016/j.watres.2014.03.054.

[35] T. Jesionowski, J. Zdarta, B. Krajewska, Enzyme immobilization by adsorption: A review, Adsorption 20 (2014) 801-821. https://doi.org/10.1007/s10450-014-9623-y.

[36] J. Zdarta, A.S. Meyer, T. Jesionowski, M. Pinelo, 2019. Multi-faceted strategy based on enzyme immobilization with reactant adsorption and membrane technology for biocatalytic removal of pollutants: A critical review. Biotechnol. Adv. 37, e107401. https://doi.org/10.1016/j.biotechadv.2019.05.007.

[37] Y. Dai, J. Yao, Y. Song, X. Liu, S. Wang, Y. Yuan, Enhanced performance of immobilized laccase in electrospun fibrous membranes by carbon nanotubes modification and its application for bisphenol A removal from water, J. Hazard. Mater. 317 (2016) 485-493. https://doi.org/10.1016/j.jhazmat.2016.06.017.

[38] R. A. Sheldon, Enzyme immobilization: The quest for optimum performance, ChemInform 38 (2007) 1289-1307. https://doi.org/10.1002/chin.200736266.

[39] Y.F. Zhang, J. Ge, Z. Liu, Enhanced activity of immobilized or chemically modified enzymes, ACS Catal. 5 (2015) 4503-4513. https://doi.org/10.1021/acscatal.5b00996.

[40] J. Wu, H. Zhang, N. Oturan, Y. Wang, Lu Chen, M. A.Oturan, Application of response surface methodology to the removal of the antibiotic tetracycline by electrochemical process using carbon-felt cathode and DSA (Ti/RuO2–IrO2) anode, Chemosphere 87 (2012) 614-620. https://doi.org/10.1016/j.chemosphere.2012.01.036.

[41] A. F. Mansor, N. A. Mohidem, W. N. Izyani, W. M. Zawawi, N. S. Othman, S. Endud, H. Mat, The optimization of synthesis conditions for laccase entrapment in mesoporous silica microparticles by response surface methodology, Micropor. Mesopor. Mat. 220 (2016) 308-314. https://doi.org/10.1016/j.micromeso.2015.08.014.

[42] K. Bachosz, K. Synoradzki, M. Staszak, M. Pinelo, A. S. Meyer, J. Zdarta, T. Jesionowski, Bioconversion of xylose to xylonic acid via co-immobilized dehydrogenases for conjunct cofactor regeneration, Bioorg. Chem. 10 (2019) 1-10. https://doi.org/10.1016/j.bioorg.2019.01.043.

[43] A. Dincer, S. Becerik, T. Aydemir, Immobilization of tyrosinase on chitosan-clay composite beads, Int. J. Biol. Macromol. 50 (201) 815-820. https://doi.org.10.1016/j.ijbiomac.2011.11.020.

[44] J. Zdarta, T. Jesionowski, Luffa cylindrica sponges as a thermally and chemically stable support for Aspergillus niger lipase, Biotechnol. Prog. 32 (2016) 657-665. https://doi.org/10.1002/btpr.2253.

[45] M. Zhang, G. Zhou, Y. Feng, T. Xiong, H. Hou, Q. Guo, Flexible 3D-nitrogen-doped carbon nanotubes nanostructure: A good matrix for enzyme immobilization and biosensing, Sensor. Actuat. B-Chem. 222 (2016) 829-838. https://doi.org/10.1016/j.snb.2015.09.030.

[46] P. Pialis, M.C.J. Hamann, B.A. Saville, L-DOPA production from tyrosinase immobilized on nylon 6,6, Biotech. Bioeng. 51 (1999) 141-147. https://doi.org/10.1002/(SICI)1097-0290(19960720)51:2<141::AID-BIT2>3.0.CO;2-J.

[47] J. Boundrant, J.M. Woodley, R. Fernandez-Lafuente, Parameters necessary to define an immobilized enzyme preparation, Process Biochem 90 (2020) 66-80. https://doi.org/10.1016/j.procbio.2019.11.026.

[48] O. Barbosa, R. Torres, C. Ortiz, R. Fernandez-Lafuente, The slow-down of the CALB immobilization rate permits to control the inter and intra molecular modification produced by glutaraldehyde, Process Biochem. 47 (2012) 766-774. https://doi.org/10.1016/j.procbio.2012.02.009.

[49] L. Fernandez-Lopez, S.G. Pedrero, N. Lopez-Carrobles, B.C. Gorines, J.J. Virgen-Ortiz, R. Fernandez-Lafuente, Effect of protein load on stability of immobilized enzymes, Enzyme Microb. Technol. 98 (2017) 18-25. https://doi.org/10.1016/j.enzmictec.2016.12.002.

[50] A.P. Minton, Influence of macromolecular crowding upon the stability and state of association of proteins: Predictions and observations, J. Pharm. Sci. 94 (2005) 1668-1675. https://doi.org/10.1002/jps.20417.

[51] S. Arana-Pena, N.S. Rios, D. Carballares, C. Mendez-Sanchez, Y. Lokha, L.R.B. Goncalves, R. Fernandez-Lafuente, 2020. Effects of enzyme loading and immobilization conditions on the catalytic features of lipase from *Pseudomonas fluorescens* immobilized on octyl-agarose beads. Front. Bioeng. Biotechnol. 8, 36. https://doi.org/10.3389/fbioe.2020.00036.

[52] M. Bilal, M. Asgher, H. Cheng, Y. Yan, H.M.N. Iqbal, Multi-point enzyme immobilization, surface chemistry and novel platforms: a paradigm shift in biocatalyst design, Crit. Rev. Biotechnol. 39 (2019) 202-219. https://doi.org/10.1080/07388551.2018.1531822.

[53] G.K. Leet, P.J. Reilly, The effect of slow intraparticle diffusion on observed immmobilized enzyme stability, Chem. Eng. Sci. 36 (1981) 1967-1975. https://doi.org/10.1016/0009-2509(81)80036-X.

[54] M. Bilal, T. Rasheed, Y. Zhao, H.M.N. Iqbal, J. Cui, "Smart" chemistry and its application in peroxidase immobilization using different support materials, Int. J. Biol. Macromol. 119 (2018) 278-290. https://doi.org/10.1016/j.ijbiomac.2018.07.134.

[55] Y.A.M. Gerritsen, C.G.J. Chapelon, H.J. Wichers, The low-isoelectric point tyrosinase of Agaricus bisporous may be a glycoprotein, Phytochemistry 35 (1994) 573-577. https://doi.org/10.1016/S0031-9422(00)90563-6.

[56] C.R. Ispas, M.T. Ravalli, A. Steere, A. Silvana, Multifunctional biomagnetic capsules for easy removal of phenol and bisphenol A, Water Res. 44 (2010) 1961-1969. https://doi.org/10.1016/j.watres.2009.11.049.

[57] M.Y. Arica, B. Altıntas, G. Bayramoglu, Immobilization of laccase onto spacer-arm attached non-porous poly(GMA/EGDMA) beads: application for textile dye degradation, Bioresour. Technol. 100 (2009) 665-669. https://doi.org/10.1016/j.biortech.2008.07.038.

[58] K.J. Laidler, P.S. Bunting, The kinetics of immobilized enzyme systems, in: D.L. Purich (Eds.), Methods in enzymology: enzyme kinetics and mechanism, DL Purich, Academic Press Inc., New York, 1980, 227-248.

[59] F. Sahin, G. Demirel, H. Tümtürk, A novel matrix for the immobilization of acetylcholinesterase, Int. J. Biol. Macromol. 37 (2005) 148-153. https://doi.org/10.1016/j.ijbiomac.2005.10.003.

[60] M.Y. Chang, R.S. Juang, Activities, stabilities, and reaction kinetics of three free and chitosan-clay composite immobilized enzymes, Enzyme Microb. Technol. 36 (2005) 75-82. https://doi.org/10.1016/j.enzmictec.2004.06.013.

[61] C.A. Staples, P.B. Dorn, G.M. Klecka, S.T. O'Block, L.R. Harris, A review of the environmental fate, effects, and exposures of bisphenol A, Chemosphere 36 (1998) 2149-2173. https://doi.org/10.1016/S0045-6535(97)10133-3.

[62] J. Zdarta, K. Antecka, R. Frankowski, A. Zgoła-Grześkowiak, H. Erlich, T. Jesionowski, The effect of operational parameters on the biodegradation of bisphenols by Trametes versicolor laccase immobilized on Hippospongia communis scaffolds, Sci Total Environ. 615 (2018) 784-795. https://doi.org/10.1016/j.scitotenv.2017.09.213.

[63] A. Yashi, F. Sakin, G. Demirel, H. Tumturuk, Binary immobilization of tyrosinase by using alginate gel beads and poly(acrylamide-co-acrylic acid) hydrogels, Int. J. Biol. Macromol. 36 (2005) 253-258. https://doi.org/10.1016/j.ibiomac.2005.06.011.

[64] R.L.O.J.L. Dias, O. Soares de Silva, A. Porto, Immobilization of pectinase from Aspergillus aculeatus in alginate beads and clarification of apple and umbu juices in a packed bed reactor, Food Bioprod. Process. 109 (2018) 9-18. https://doi.org/10.1016/j.fbp.2018.02.005.

[65] A. Tamura, E. Satoh, A. Kashiwada, K. Matsuda, K. Yamada, Removal of alkylphenols by the combined use of tyrosinase immobilized on ion-exchange resins and chitosan beads, J. Appl. Polym. Sci. 115 (2010) 137-145. https://doi.org/10.1002/app.30947.

[66] C. Nicolucci, S. Rossi, C. Menale, T. Godjevargova, Y. Ivanov, M. Bianco, L. Mita, U. Bencivenga, D.G. Mita, N. Diano, Biodegradation of bisphenols with immobilized laccase or tyrosinase on polyacrylonitrile beads, Biodegradation 22 (2011) 673-683. https://doi.org/10.1007/s10532-010-9440-2.

[67] M.E. Marin-Zamora, F. Rojas-Melgarejo, F. Garcia-Canovas, P.A. Garcia-Ruiz, Effects of the immobilization supports on the catalytic properties of immobilized mushroom tyrosinase: A comparative study using several substrates, J. Biotechnol. 131 (2007) 388-396. https://doi.org/10.1016/j.jbiotec.2007.05.004.

[68] W.T. Ismaya, H.J. Rozeboom, A. Weijn, J.J. Mes, F. Fusetti, H.J. Wichers, B.W. Dijkstra, Crystal structure of Agaricus bisporus mushroom tyrosinase: identity of the tetramer subunits and interaction with tropolone, Biochemistry 50 (2011) 5477-5486. https://doi.org/10.1021/bi200395t.

[69] G. Bayramoglu, M.Y. Arica, Reversible immobilization of catalase on fibrous polymer grafted and metal chelated chitosan membrane, J. Mol. Catal. B: Enzym. 62 (2010) 297-304. https://doi.org/10.1016/j.molcatb.2009.11.013.

[70] Q. Wu, Z. Xu, Y. Duan, Y. Zhu, M. Ou, X. Xu, Immobilization of tyrosinase on polyacrylonitrile beads: biodegradation of phenol from aqueous solution and the relevant cytotoxicity assessment, RSC Advances 7 (2017) 28114-28123. https://doi.org/10.1039/C7RA03174B.

[71] K. Abollahi, F. Yazdani, R. Panahi, Fabrication of the robust and recyclable tyrosinase-harboring biocatalyst using ethylenediamine functionalized superparamagnetic nanoparticles: nanocarrier characterization and immobilized enzyme properties, J. Biol. Inorg. Chem. 24 (2019) 943-959. https://doi.org/10.1007/s00775-019-01690-1.

[72] J. Shao, H. Ge, Y. Yang, Immobilization of polyphenol oxidase on chitosan–SiO_2 gel for removal of aqueous phenol, Biotechnol. Lett. 29 (2007) 901-905. https://doi.org/10.1007/s10529-007-9329-2.

[73] G. Bayramoglu, M. Yilmaz, M.Y. Arica, Preparation and characterization of epoxy-functionalized magnetic chitosan beads: Laccase immobilized for degradation of reactive dyes, Bioprocess Biosyst. Eng. 33 (2010) 439-448. https://doi.org/10.1007/s00449-009-0345-6.

[74] S.A. Cetinus, H.N. Oztop, Immobilization of catalase into chemically crosslinked chitosan beads, Enzyme Microb. Technol. 32 (2003) 889-894. https://doi.org/10.1016/S0141-0229(03)00065-6.

[75] J. L. Gomez, A. Bodalo, E. Gomez, J. Bastida, A. M. Hidalgo M. Gomez, Immobilization of peroxidases on glass beads: An improved alternative for phenol removal, Enzyme Microb. Technol. 39 (2006) 1016-1022. https://doi.org/10.1016/j.enzmictec.2006.02.008.

[76] G. Bayramoglu, B. Altintas, M. Yilmaz, M. Y. Arica, Immobilization of chloroperoxidase onto highly hydrophilic polyethylene chains via bio-conjugation: Catalytic properties and stabilities, Bioresour. Technol. 102 (2011) 475-482. https://doi.org/10.1016/j.biortech.2010.08.056.

[77] E. Arkan, C. Karami, R. Rafipur, Immobilization of tyrosinase on Fe3o4@Au core–shell nanoparticles as bio-probe for detection of dopamine, phenol and catechol, J. Biol. Inorg. Chem. 24 (2019) 961-969. https://doi.org/10.1007/s00775-019-01691-0.

[78] D. Dodor, H. Hwang, E. Sin, Oxidation of anthracene and benzo[a]pyrene by immobilized laccase from Trametes versicolor, Enzyme Microb. Technol. 35 (2004) 210-217. https://doi.org/10.1016/j.enzmictec.2004.04.007.

[79] C. Ji, L.N. Nguyen, J. Hou, F.I. Hai, V. Chen, Direct immobilization of laccase on titania nanoparticles from crude enzyme extracts of P. ostreatus culture for micropollutant degradation, Sep. Purif. Technol. 178 (2017) 215-223. http://dx.doi.org/10.1016/j.seppur.2017.01.043.

[80] F.A.D. Inroga, M.O. Rocha, V. Lavayen, J. Arguello, Development of a tyrosinase-based biosensor for bisphenol A detection using gold leaf–like microstructures, J. Solid State Electr. 23 (2019) 1659-1666. https://doi.org/10.1007/s10008-019-04252-2.

[81] M. Bilal, H.M.N. Iqbal, H. Hu, W. Wang, X. Zhang, Enhanced bio-catalytic performance and dye degradation potential of chitosan-encapsulated horseradish peroxidase in a packed bed reactor system, Sci. Total Environ. 575 (2017) 1352-1360. https://doi.org/10.1016/j.scitotenv.2016.09.215.

[82] A. Veismorandi, S.M. Mousavi, M. Taherian, Decolorization of dye solutions by tyrosinase in enzymatic membrane reactors, J. Chem. Technol. Biotechnol. 94 (2019) 3559-5568. https://doi.org/10.1002/jctb.6158.

Table 1. Calculated parameters of models *F* for selected relations between explanatory (measured) variables *A* and *B*.

A	*B*	a_1	a_2	a_3	a_4	a_5	a_6	A_{opt}	B_{opt}	R^2	Std. dev.
pH	***t, min***	-111.80	39.404	4.226	0.234	-2.631	-0.146	8.433	21.187	0.944	6.598
pH	***C, g/L***	-128.46	40.853	37.696	0.363	-2.616	-5.874	8.048	3.458	0.906	8.814
pH	***T, °C***	-145.20	53.332	1.956	-0.043	-3.265	-0.024	7.946	33.669	0.979	3.163
T, °C	***C, g/L***	8.57	1.483	39.145	-0.0050	-0.02	-5.532	36.064	3.522	0.891	8.202
T, °C	***t, min***	4.592	1.774	7.001	-0.0037	-0.025	-0.188	33.725	18.294	0.96	5.19
C, g/L	***t, min***	4.303	27.46	4.631	0.326	-4.749	-0.146	3.57	19.78	0.893	8.842

Figure captions:

Fig. 1. Scheme presenting fabrication of polycaprolactone–chitosan (PCL–chitosan) electrospun material and immobilization process carried out in this study, with detail insight into mechanism of performed process.

Fig. 2. SEM images of the PCL-chitosan electrospun materials before (a) and after (b) enzyme immobilization.

Fig. 3. Response surface for catalyst activity in function of pH and process time. Dot indicate rescaled experimental values.

Fig. 4. Immobilization course of tyrosinase onto PCL-chitosan electrospun support material. Immobilization was performed at pH 7 and 25 °C using enzyme solution at concentration 3 mg/mL.

Fig 5. Time course of the removal of BPA by free and immobilized tyrosinase (a) and effect of: initial BPA concentration (b), process temperature (c) and pH of the solution (d) on the removal efficiency of BPA by free and immobilized tyrosinase.

Fig. 6. Storage stability (a) and thermochemical stability (b) of the free and PCL-chitosan immobilized tyrosinase and reusability (c) of the immobilized enzyme over repeated reaction cycles.

Figure 1

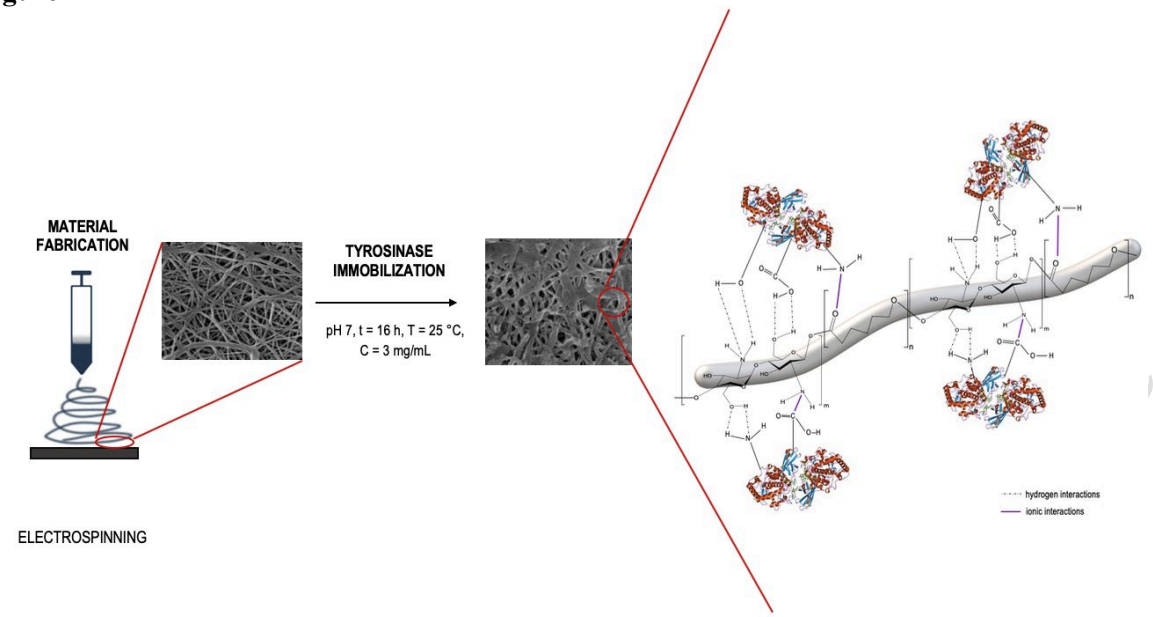

International Journal of Biological Macromolecules, Zdarta et al.

Figure 2

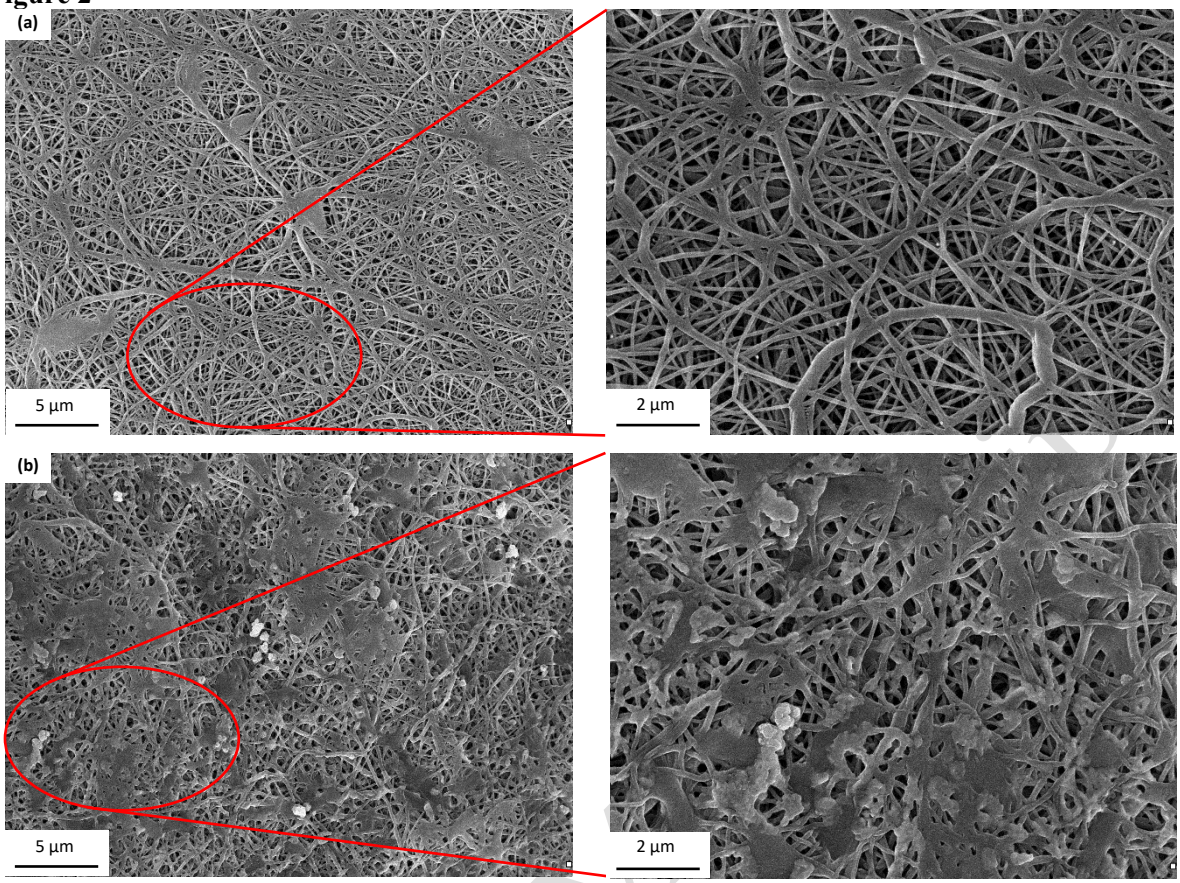

International Journal of Biological Macromolecules, Zdarta et al.

Figure 3

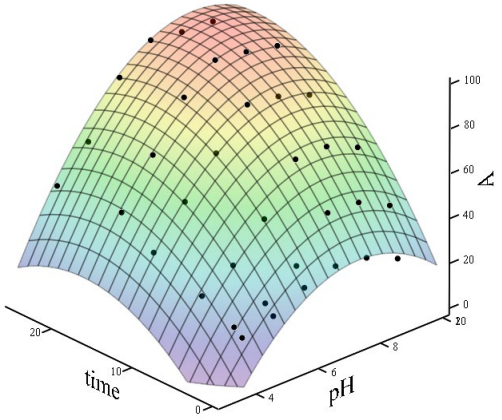

International Journal of Biological Macromolecules, Zdarta et al.

Figure 4

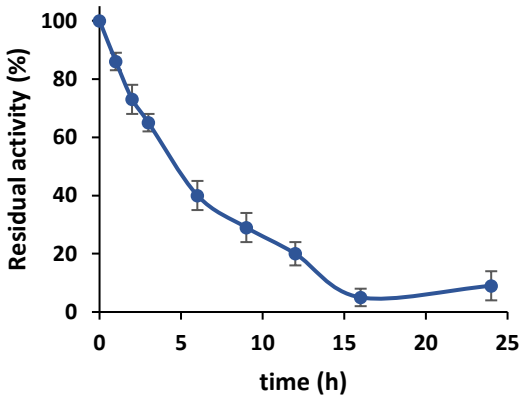

International Journal of Biological Macromolecules, Zdarta et al.

Figure 5

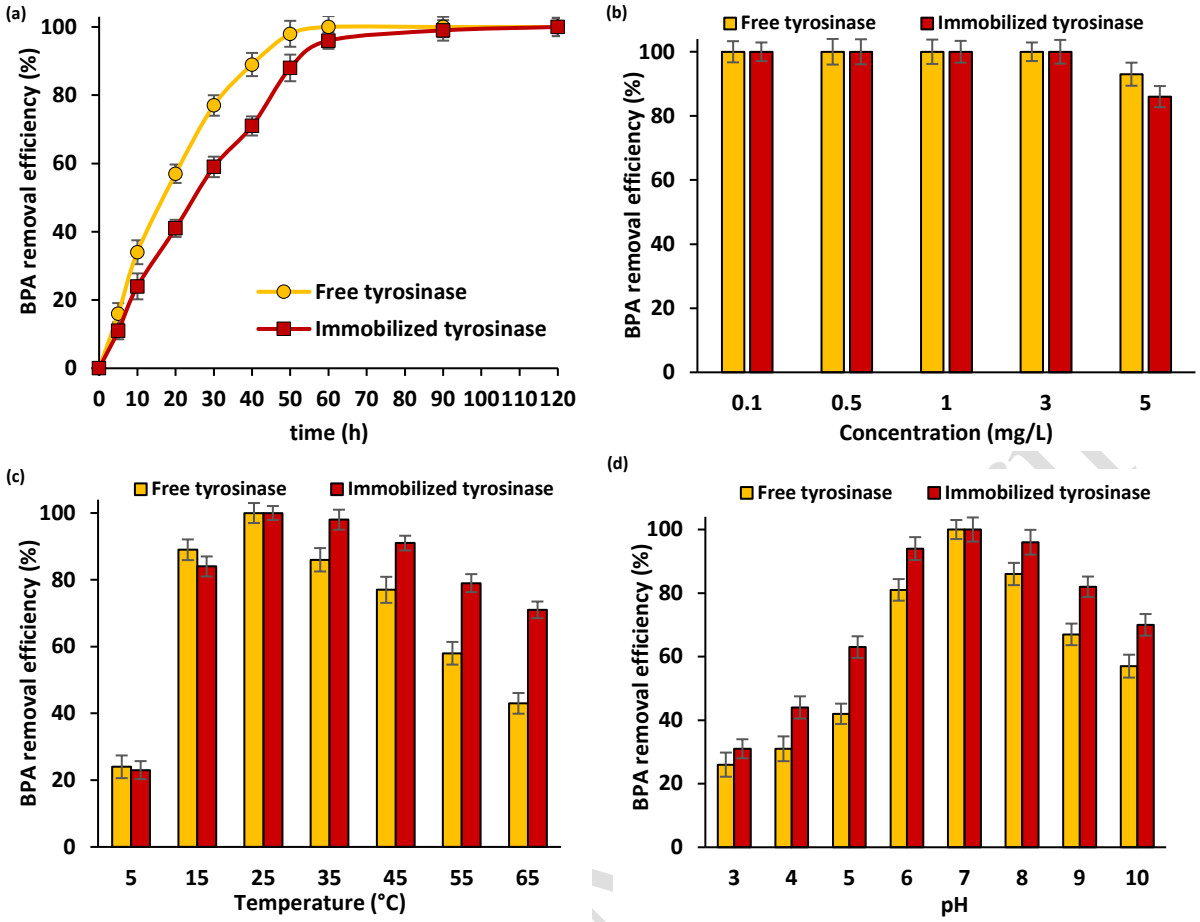

International Journal of Biological Macromolecules, Zdarta et al.

Figure 6